

Ferrimagnetic ordering of one-dimensional N,N' -dicyanoquinone diimine (DCNQI) electron transfer salts with porphyrinatomanganese(II)†

Ken-ichi Sugiura,^{*a,‡} Shinji Mikami,^a Mitchell T. Johnson,^b James W. Raebiger,^b Joel S. Miller,^{*b} Kentaro Iwasaki,^c Yuko Okada,^c Shojun Hino^c and Yoshiteru Sakata^{*a}

^aThe Institute of Scientific and Industrial Research (ISIR), Osaka University, 8-1 Mihogaoka, Ibaraki, Osaka 567-0047, Japan. E-mail: sugiura@comp.metro-u.ac.jp; sakata@sanken.osaka-u.ac.jp

^bDepartment of Chemistry, University of Utah, Salt Lake City, UT 84112-0850, USA. E-mail: jsmiller@chemistry.utah.edu

^cFaculty of Engineering, Chiba University, Inageku, Chiba 263-8522, Japan

Received 26th January 2001, Accepted 16th May 2001

First published as an Advance Article on the web 12th June 2001

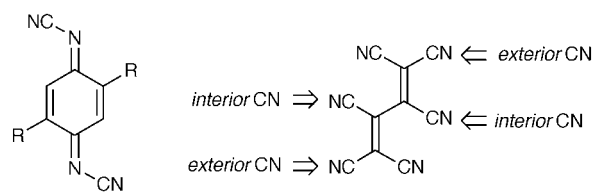
The redox reaction between N,N' -dicyanoquinone diimines (DCNQIs) and porphyrinatomanganese(II) produced electron transfer salts (ETSs), $[\text{Mn}^{\text{III}}\text{TMeSP}]^+ [\text{DMeO-DCNQI}]^-$ **1** ($\text{Mn}^{\text{III}}\text{TMeSP} = \text{meso-tetrakis}(2,4,6\text{-trimethylphenyl})\text{porphyrinatomanganese(III)}$, $\text{DMeO-DCNQI} = 2,5\text{-dimethoxy-}N,N'\text{-dicyanoquinone diimine}$) and $[\text{Mn}^{\text{III}}\text{TMeSP}]^+ [\text{DMe-DCNQI}]^-$ **2** ($\text{DMe-DCNQI} = 2,5\text{-dimethyl-}N,N'\text{-dicyanoquinone diimine}$), having uniform chain structures that have been structurally and magnetically characterised. The salts have infinite one-dimensional linear chains comprised of $S=2$ $[\text{Mn}^{\text{III}}\text{TMeSP}]^+$ and bridging $S=\frac{1}{2}$ $[\text{DCNQIs}]^-$ with $\text{Mn-N}^{\text{DCNQIs}}$ distances of 2.249(2) and 2.261(4) Å for **1** and **2**, respectively. The temperature dependence of the magnetic susceptibility from 2 to 300 K can be fitted to a Curie–Weiss expression with an effective θ value of +41 and +23 K for **1** and **2**, respectively. Intrachain coupling was modelled to a Seiden expression ($H = -2J_{ij}S_i \cdot S_j$) with a J_{intra} of -90 (**1**) and -50 K (**2**), and the 10 Hz ac magnetic susceptibility indicates an ordering temperature, T_c , of 6.2 and 6.0 K for **1** and **2**, respectively. The frequency dependencies of the ac susceptibility indicate spin glass behaviour.

Introduction

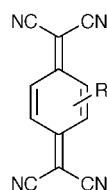
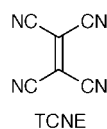
The discovery of the N,N' -dicyanoquinone diimine, DCNQI, family of strong electron acceptor molecules by Hünig and Aumüller in 1984¹ has led to the development of a large variety of highly conducting materials.² In particular, mixed valence copper salts have provided a rich science such as metallic conductivity without Peierls transitions,² re-entrant second-order phase transitions enhanced by the deuterium isotope effect,³ and a three-dimensional Fermi surface observed for the first time for a molecule-based conductor.⁴ These characteristic features are attributed to the cooperative $d\pi\text{-}p\pi^*$ interaction between $\text{Cu}^{1.3+}$ and partially reduced DCNQI ligands.^{2,5} DCNQIs can also act as a magnetic scaffold for the localised electrons, *i.e.*, net magnetic exchange interactions between the d -electrons of the transition metals through DCNQIs. Such interactions are observed in non-covalent⁶ and coordinative systems.⁷ For the latter, Crutchley and Kaim *et al.* systematically reported Creutz–Taube type mixed valence ruthenium complexes bridged by DCNQI dianions.⁷ The antiferromagnetic interactions of these complexes *via* the hole exchange mechanism⁷ are extremely large, *e.g.*, $J \geq -575$ K (~ -400 cm^{-1}) (*vide infra*).⁸

We have developed a family of molecule-based magnets:⁹ electron transfer salts (ETSs) comprised of porphyrinatomanganese(II) $[\text{Mn}^{\text{II}}\text{P}]$ and cyanocarbon acceptors such as tetracyanoethylene (TCNE),⁹ 7,7,8,8-tetracyano-*p*-quinodimethanes

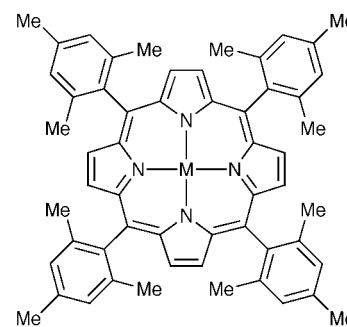
(TCNQs),^{10–12} and hexacyanobutadiene (HCBD).^{13–17} These ETSs have extended one-dimensional (1-D) chain structures with coordination bonds between Mn^{III} and nitrogen atoms of acceptor molecules. Their magnetic exchange interactions ($J \approx -200$ K) are strong¹⁸ with exceptionally large coercive fields at 2 K, behaviour which is comparable to that of commercially used rare earth magnets ($H_{\text{cr}} \approx 2.7$ T).¹⁹



DCNQI (R = H)
DMeO-DCNQI (R = OMe)
DMe-DCNQI (R = Me)



TCNQs (R = H, Me, F)



$\text{Mn}^{\text{II}}\text{TMeSP}$ (M = Mn^{II})
 $[\text{Mn}^{\text{III}}\text{TMeSP}]^+$ (M = Mn^{III})

†Electronic supplementary information (ESI) available: Figs. S1–S6. See <http://www.rsc.org/suppdata/jm/b1/b100936m/>

‡Present address: Department of Chemistry, Graduate School of Science, Tokyo Metropolitan University, 1-1Minami-ohsawa, Hachioji, Tokyo 192-0397, Japan. E-mail: sugiura@comp.metro-u.ac.jp; Fax: +81-426-77-2525; Tel: +81-426-77-2551.

In the course of our studies, we have discovered that a large spin density on the bonding site of the bridging ligand is needed for a large spin exchange interaction. For example, *exterior* coordinated [HCBD][−] ETSSs, with the Mn^{III} bound to the *exterior* CN groups having large spin density, display strong antiferromagnetic interactions,^{13–15,17} whereas, *interior* coordinated [HCBD][−] ETSSs, with the Mn^{III} bound to the *interior* CN groups having small spin density, display weak exchange interactions.^{16,17} Furthermore, closed shell bridging ligands only produce paramagnetic ETSSs.²⁰ These results are in marked contrast to Crutchley's results as described above.⁸

In order to explore the exchange interaction for the paramagnetic metal complexes bridged by [DCNQIs][−], we studied the [Mn^{III}P]⁺[DCNQIs][−] system. This study will also lead to new coordination chemistry for these acceptors, and moreover, open new materials chemistry such as a molecule-based magnetic metals showing both magnetic ordering and metallic conductivity.⁵ Herein, we report the synthesis and characterisation of the ETSSs of *meso*-tetrakis(2,4,6-trimethylphenyl)porphyrinatomanganese(II) (Mn^{II}TmesP) with 2,5-dimethoxy-*N,N'*-dicyanoquinone diimine (DMeO-DCNQI) and 2,5-dimethyl-*N,N'*-dicyanoquinone diimine (DMe-DCNQI), which are the first examples of 1-D ionic coordinated μ -[DCNQIs][−].

Result and discussion

Synthesis and spectroscopic studies

Direct redox reactions of Mn^{II}TmesP with DMeO-DCNQI and DMe-DCNQI²¹ were performed under an inert atmosphere to give dark coloured 1:1 complexes, [MnTmesP]-[DMeO-DCNQI], **1**, and [MnTmesP][DMe-DCNQI], **2**, respectively. Although the ETSSs of DCNQIs with organic donor molecules tend to produce non-integral numbers of D:A stoichiometry,²² those of **1** and **2** were determined to be 1:1 on the basis of elemental and crystal structure analyses (*vide infra*).

The degree of charge transfer for **1** and **2** was determined by IR and X-ray photoelectron spectroscopic (XPS) as well as

magnetic studies (*vide infra*). The ν_{CN} absorptions for the former (**1**: 2116 cm^{−1}) and the latter (**2**: 2103 cm^{−1}) showed band shifts by −59 and −65 cm^{−1}, respectively, compared with the corresponding values of neutral [DMeO-DCNQI]⁰ (2175 cm^{−1}) and [DMe-DCNQI]⁰ (2168 cm^{−1})²³ (Table 1 and electronic supplementary information (ESI) as Fig. S1). These values are also shifted to lower energy compared with those of the ETSSs with partial electron transfer, *e.g.*, the corresponding tetrathiafulvalene (TTF)-based ETSSs, 2150 cm^{−1} for [TTF][DMeO-DCNQI]²⁴ and 2140 cm^{−1} for [TTF][DMe-DCNQI]^{24,25} and are shifted to higher energy than those for the dianion, *e.g.*, 2093 cm^{−1} for [DMe-DCNQI]^{2−}.²⁶ The values of **1** and **2** are comparable to that for the anion radical, *e.g.*, 2118 cm^{−1} for [DMe-DCNQI][−].²³ Thus, the [DCNQIs]⁰ are reduced to [DCNQIs][−] by Mn^{II}TmesP. The frequency shift arising from back-bonding expected for Mn^{II}-NC coordination is small,^{27,28} *e.g.*, −13 cm^{−1} for **2**. The broad band shapes of the ν_{CN} absorptions are frequently observed for coordinative DCNQI ETSSs.²⁴

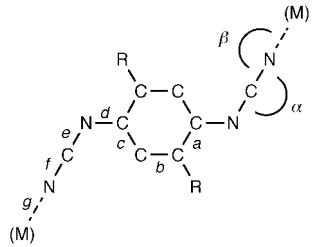
Other marker bands reflecting the ionicity of the DCNQIs,^{23,29} $\nu_{\text{C-N}}$ and $\nu_{\text{C-C}}$ stretching modes having IR-active b_u symmetries also support the ionic ground states of **1** and **2** (Table 1 and ESI, Fig. S1).

XPS also supports the one electron oxidation of Mn^{II} (Fig. 1 and Table 2). Thus, the core ionisation potentials for manganese, Mn2p_{3/2} and Mn2p_{1/2}, of **1** (642.5 and 654.0 eV) and **2** (642.6 and 654.2 eV) are nearly identical to those of six-coordinated Mn^{III} (642.6 and 654.2 eV for [Mn^{III}TPP]⁺-[TCNE][−]·2PhMe).³⁰ The IR and XPS results clearly indicate the formation of *S*=2 for [Mn^{III}TmesP]⁺ and *S*= $\frac{1}{2}$ for the [DCNQIs][−].

Structure

The crystal structures of **1** and **2** are shown in Fig. 2 and some important structural parameters of the ETSSs are summarised in Table 1 together with the data of several reference complexes including neutral DMeO-DCNQI (the structure of neutral DMeO-DCNQI is shown in the ESI, Fig. S2). The [DCNQIs][−]

Table 1 Spectroscopic and structural parameters for **1**, **2**, and reference compounds/complexes



	1	DMeO-DCNQI	[TTF][DMeO-DCNQI]	Cu[DMeO-DCNQI] ₂	2	DMe-DCNQI	[TTF][DMe-DCNQI]	[Mo ₂ (O ₂ CCF ₃) ₄][DMe-DCNQI]	Cu[DMe-DCNQI] ₂	[AsPh ₄] ₂ [DMe-DCNQI] ^{2−}
Ionicity	Ionic	Neutral	Partial	Partial	Ionic	Neutral	Neutral	Neutral	Partial	Dianion
$\nu_{\text{CN}}/\text{cm}^{-1}$	2116	2175	2150	Unknown	2103	2168	2140	2230		2118
Bond										
<i>a</i> /Å	1.437(3)	1.481(3)		1.452	1.435(6)	1.473	1.463(4)	1.461	1.441	1.406
<i>b</i> /Å	1.364(3)	1.361(3)		1.352	1.352(5)	1.342	1.342(4)	1.369	1.362	
<i>c</i> /Å	1.411(3)	1.440(3)		1.413	1.428(6)	1.447	1.449(4)	1.440	1.435	
<i>d</i> /Å	1.350(3)	1.311(3)		1.335	1.359(5)	1.319	1.308(3)	1.317	1.334	1.408
<i>e</i> /Å	1.306(3)	1.334(3)		1.321	1.309(6)	1.350	1.340(4)	1.368	1.311	1.32
<i>f</i> /Å	1.156(3)	1.150(3)		1.150	1.163(6)	1.148	1.147(4)	1.146	1.159	1.15
<i>g</i> /Å	2.249(2)			1.988	2.261(4)			2.531	1.969	
α°	175.9(2)	173.0(2)			173.1(4)	172.8	172.9(3)	173.1	172.8	
β°	150.7(2)				158.4(4)			140.1	170.6	
<i>T</i> /K	223	224		RT		RT	RT	104	100	295
Reference	This work	This work	24	33a	This work	25	24, 25	44	33a	26, 48

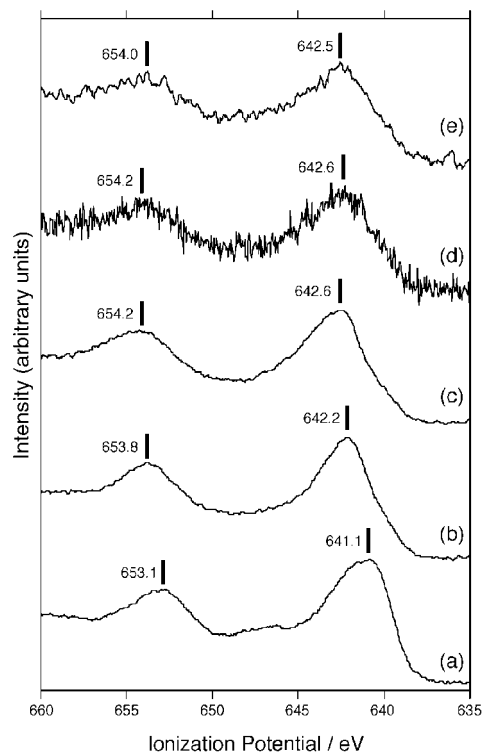


Fig. 1 The Mn 2p XPS of (a) $[\text{Mn}^{\text{II}}\text{TPP}] \cdot \text{pyridine}$, (b) $[\text{Mn}^{\text{III}}\text{TPP}]^+ \text{Cl}^-$, (c) $[\text{Mn}^{\text{III}}\text{TPP}]^+ [\text{TCNE}]^-$, (d) **2**, and (e) **1**.

bond lengths of **1** and **2** differ significantly from those for neutral DCNQIs and the ETS having neutral ground states. The key distances that best describe the oxidation state of the DCNQIs are the *exo*-methylene bond (*d* in inset figure of Table 1). The distances of these bonds are 1.350(3) Å for **1** and 1.359(5) Å for **2** and are ~ 0.04 Å longer than those for neutral DCNQIs, *i.e.*, 1.311(3) Å for DMeO-DCNQI and 1.319(5) Å for DMe-DCNQI.²⁵ These quinone-type bonds become longer with an increase of negative charge in $[\text{DCNQI}]^{n-}$ ($n=1, 2$). The increase in negative charge also results in a contraction of bonds *a* and *c* and a lengthening of bond *b*. These changes are attributable to the development of aromatic character in the central six-membered ring after electron transfer. Hence, in accord with the $\nu_{\text{C}=\text{N}}$, $\nu_{\text{C}-\text{N}}$, and $\nu_{\text{C}=\text{C}}$ absorptions, as well as the XPS data (*vide supra*), the species $[\text{DCNQI}]^{n-}$ are present in these complexes. The bond length of the cyanoimine moiety may also reflect the ionicity of the DCNQIs, *i.e.*, bond *e* and bond *f* are intermediate values between those for the neutral and dianionic species.

Although both the nitrile² and imine nitrogen atoms³¹ of the DCNQIs are able to coordinate to the metal ions, only the terminal nitrogen atoms of the nitrile are bound to Mn^{III} . Both DCNQIs and Mn^{III} are located on the inversion centres and produce infinite uniform 1-D chain structures, as observed for $[\text{MnP}][\text{TCNE}]_s$.⁹ This is in contrast to the non-bonded π -stacking,¹⁷ uniform *zig-zag*,^{12,17} and non-uniform *zig-zag*

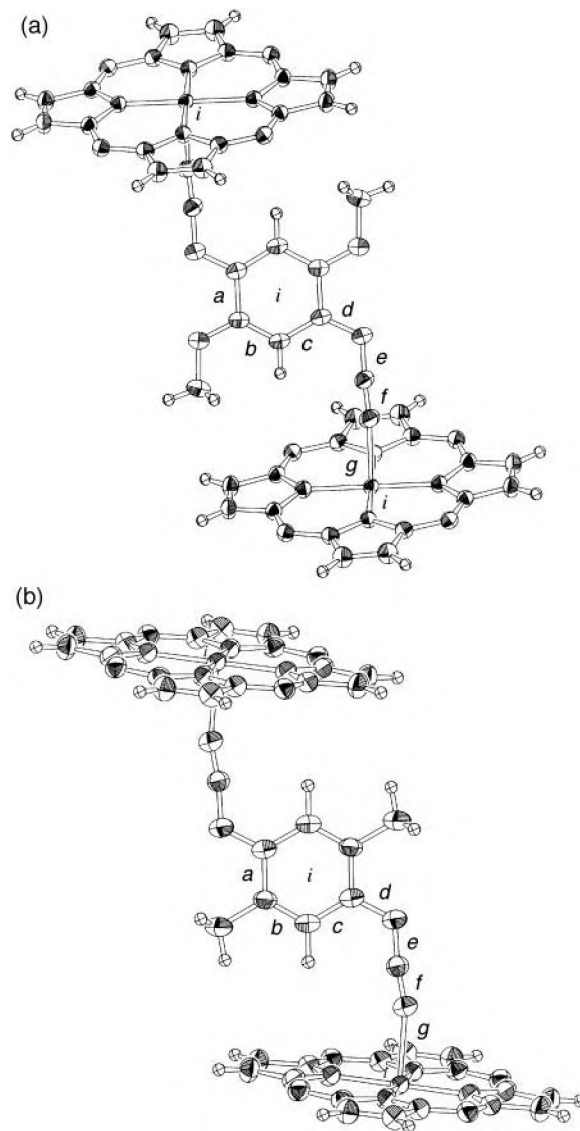


Fig. 2 ORTEP drawings of (a) **1** and (b) **2**. Thermal ellipsoids are 50% probability levels. Mesityl groups of $[\text{Mn}^{\text{III}}\text{TmesP}]^+$ and solvent molecules are omitted for clarity. Both Mn^{III} and DCNQIs are located on the inversion centre (*i*).

chains.^{10,11,13,17,32} frequently observed for the $[\text{Mn}^{\text{III}}\text{P}]^+ [\text{acceptor}]^-$ system based on π -expanded acceptor molecules such as TCNQs and HCBP. The Mn–N bond lengths ($d_{\text{Mn}-\text{N}^{\text{DCNQIs}}}$) are 2.249(3) and 2.261(4) Å for **1** and **2**, respectively. These values are comparable to those observed for $[\text{MnP}][\text{TCNE}]_s$ (2.2 to 2.5 Å),⁹ and are much longer than those observed for $d\pi$ - π^* and/or $d\pi$ - π^{HOMO} orbital overlapped systems, *e.g.*, $d_{\text{Cu}-\text{N}^{\text{DCNQIs}}}$ (1.94 to 1.99)^{2,33} and $d_{\text{Ru}-\text{N}^{\text{DCNQIs}}}$ (1.94 to 1.99 Å),^{8,34,35} which suggests that the $[\text{Mn}^{\text{III}}\text{P}]^+ [\text{DCNQIs}]^-$ system lacks $d\pi$ - π^* and/or $d\pi$ - π^{HOMO} orbital interactions. The $d_{\text{Mn}-\text{N}^{\text{DCNQIs}}}$ of **1** and **2** suggest the presence of d_{z^2} - π^* orbital interactions (*vide infra*).³⁶ The Mn–NC^{DCNQIs} angles ($\angle \text{MnNC}$) and the dihedral angle between the MnN4 porphyrin and $[\text{DCNQI}]^{n-}$ planes are 150.7(2) and 61.9(1)° for **1** and 158.4(4) and 79.1(1)° for **2**, respectively. These parameters are considered to be important for the magnetic coupling pathway.³⁶ Due to these large dihedral angles and the large size of the DCNQIs, compared to TCNE, the porphyrin–porphyrin interplanar distances ($d_{\text{P}-\text{P}}$) and the intrachain Mn...Mn distances ($d_{\text{Mn}-\text{Mn}} \equiv a$ -axis) are larger, *i.e.*, 11.34 and 12.795(2) Å for **1**, and 11.24 and 12.988(5) Å for **2**, respectively. These values are significantly larger than the corresponding values for $[\text{MnP}][\text{TCNE}]_s$, which

Table 2 XPS core IPs (eV) for **1**, **2**, and related compounds^a

	C1s	N1s	Mn2p _{3/2}	Mn2p _{1/2}	Reference
1	285.0	398.9	642.5	654.0	This work
2	285.0	399.1	642.6	654.2	This work
$[\text{Mn}^{\text{III}}\text{TPP}]^+$	284.9	399.1	642.6	654.2	30
$[\text{TCNE}]^- \cdot 2\text{PhMe}$	284.9	398.9	642.2	653.8	30
$[\text{Mn}^{\text{III}}\text{TPP}]^+ \text{Cl}^-$	284.9	398.4	641.1	653.1	30

^aThe spectrometers were calibrated such that the Au 4f_{7/2} peak of the clean sputtered metals appeared at 84.0 eV. IPs are reproducible to a precision of $\leq \pm 0.10$ eV.

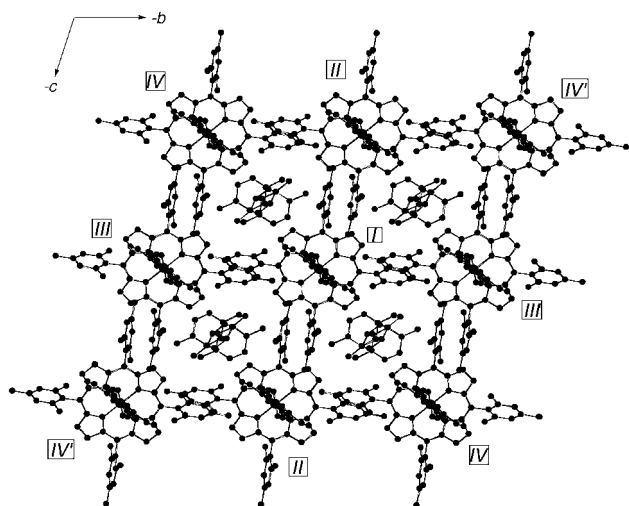


Fig. 3 Top view of the crystal packing of **1**. Solvent molecules, *p*-xylene, are shown in black circles.

range from 7.0 to 10.0 Å for *d*P-P, and 9.5 to 10.5 Å for *d*Mn-Mn.⁹

The packing structures are shown in Figs. 3 and 4 for **1**. The 1-D chain (Chain-I; Figs. 3 and 4) is surrounded by the two nearest neighbouring chains (Chains-II) in the [001] ($\equiv c$ -axis) direction and by the next neighbouring two chains (Chains-IV) in the [010] ($\equiv b$ -axis) direction. These 1-D chains produce a large pore in the [100] ($\equiv a$ -axis) direction and the solvent

molecules are incorporated in these channels. The bulky mesityl (2,4,6-trimethylphenyl) groups prevent the formation of a 2-D sheet structure, which is usually seen in the unsubstituted TPP based [MnP][TCNE] systems, in which a 2-D structure is produced by the weak interactions between [TCNE]⁻ and the phenyl group of TPP of the adjacent 1-D chains.³⁷ There exists no such mesityl-DCNQI π -overlapping for **1**. The packing motif of **1** is similar to that observed for [Mn^{III}T^tBuPP]⁺[TCNE]⁻·*6p*-xylene.³⁸ This may be attributable to the steric effects both of DCNQIs and of the methyl groups introduced into the TPP ligand. Chains-II and -III interact with Chain-I in *in-registry* and *out-of-registry* manners, respectively.³⁹ Interchain interactions such as the shortest Mn-Mn (12.04 Å with Chain-II, 14.08 and 15.19 Å with Chain-III) and Mn-[DMeO-DCNQI]⁻ (13.19 and 14.19 Å with Chain-II, 13.23 Å with Chain-III) are similar to those for the [Mn^{III}P]⁺[TCNE]⁻ systems, 11.006 to 14.932 Å (Fig. 4). Although the crystal symmetry is different, *P*₂/*c*, **2** has a similar gross molecular alignment to **1** (ESI, Figs. S3–S5).

Magnetic behaviour

The susceptibilities (χ) of **1** and **2** were measured between 2 and 300 K and can be fitted to the Curie-Weiss equation, $\chi = 1/(T - \theta)$, with a θ of +40.7 K ($40 < T < 175$ K) for **1**, -17.1 K ($T > 170$ K) and effective θ' of +23.4 ($40 < T < 120$ K) for **2**, respectively, indicating long range ferromagnetic coupling (Fig. 5). These θ values are close to the reported values observed for [MnP][TCNE] with uniform chains in the range of 12 to 100 K.⁹ The larger θ value of **1** (+47 K) as

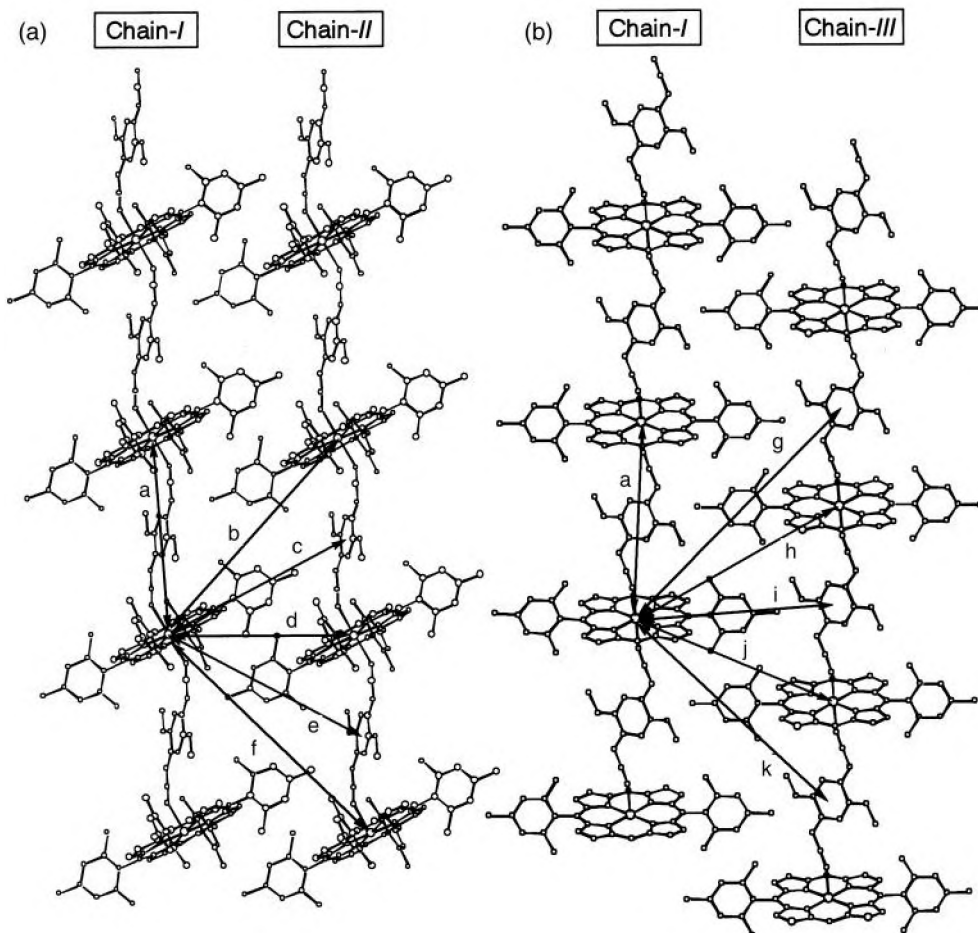


Fig. 4 Views of the interchain interactions among the unique chains of **1**: (a) Chain-I and Chain-II; (b) Chain-I and Chain-III [all the hydrogen atoms are omitted for clarity and the front mesityl groups in (b) have also been removed]. The important interactions are the followings: $a = 12.795$ ($\equiv a$ -axis), $b = 16.774$, $c = 13.186$, $d = 12.042$ ($\equiv c$ -axis), $e = 14.189$, $f = 18.331$, $g = 19.266$, $h = 15.193$, $i = 13.230$, $j = 14.082$ ($\equiv b$ -axis), and $k = 17.490$ Å.

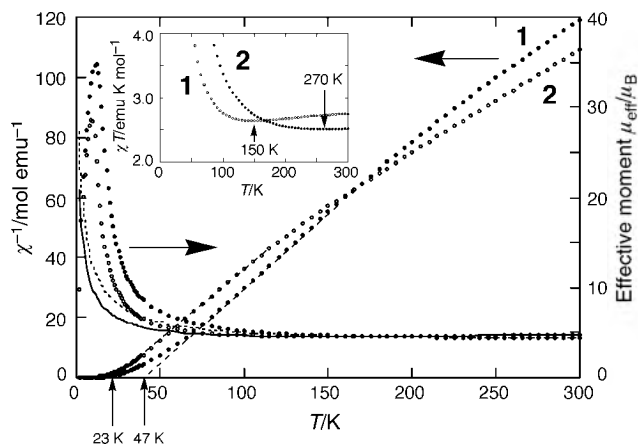


Fig. 5 $\chi^{-1}(T)$ and the effective moment $\mu_{\text{eff}}(T)$ for **1** (●) and **2** (○). The dotted lines are the fit of $\chi^{-1}(T)$ to the Curie–Weiss equation with $\theta = 41$ and 23 K for **1** and **2**, respectively. The solid and dotted lines are the fit of $\mu_{\text{eff}}(T)$ to the Seiden expression with $J/k_{\text{B}} = -90$ and -50 K for **1** and **2**, respectively. Inset is $\chi(T)$ plot of **1** (●) and **2** (○).

compared with that of **2** (+23 K) is consistent with the correlation between $\angle\text{MnNC}$ and θ observed for TCNE ETSS.³⁶ The minimum in $\chi T(T)$ characteristic of 1-D antiferromagnetic coupling was observed at 270 and 150 K for **1** and **2**, respectively (inset of Fig. 5).⁴⁰

When the temperature was decreased, $\mu_{\text{eff}}(T)$ reached a maximum value of 34.7 (at 14 K for **1**) and 28.6 μ_{B} (at 9 K for **2**) due to saturation. The room temperature effective moment values, $\mu_{\text{eff}} [(8\chi T)^{-1/2}]$ are 4.48 (**1**) and 4.68 μ_{B} (**2**) and are lower than the predicted values for independent isotropic $g=2$, $S=2$ of Mn^{III} and $S=\frac{1}{2}$ of $[\text{DCNQI}]^{\cdot-}$ spin systems (5.20 μ_{B}). These reduced values are due to antiferromagnetic coupling.

The intrachain coupling, J , can be determined from a fit of $\chi T(T)$ to the Seiden model⁴¹ for non-interacting chains comprised of alternating $g=2$, quantum, $S=2$ and classical $S=\frac{1}{2}$ spins. The data can be fitted to the Seiden expression above 70 K with $J/k_{\text{B}} = -90$ (for **1**) and -50 K (for **2**) for $\mathbf{H} = -2J_{ij}\mathbf{S}_i\cdot\mathbf{S}_j$, as shown in Fig. 5. The negative J value reflects the strong intrachain antiferromagnetic coupling and the value of **1** is almost twice as large as that for **2** with respect to **2**. This is attributable to the smaller $\angle\text{MnNC}$ of **1** (*vide supra*). Below 70 K, the observed $\chi T(T)$ exceeds the values predicted from the Seiden model, indicating that the ferromagnetic coupling between chains begins to dominate. This has also been observed for other members of the $[\text{MnP}][\text{TCNE}]$ family of magnets and is attributed to ferromagnetic interaction arising from dipolar coupling.³⁷

The ferrimagnetic nature of this system may also be realised from the magnetisation values at 2 K and 50 kOe. The data for **1** (14200 emu Oe mol⁻¹) and **2** (10200 emu Oe mol⁻¹) are consistent with an antiferromagnetically coupled $S_{\text{tot}} = 2 - \frac{1}{2} = \frac{3}{2}$ system, *cf.*, an expected saturation magnetisation, M_{s} , of 16755 emu Oe mol⁻¹, and are substantially lower than expectation for ferromagnetic coupling, *cf.*, an M_{s} of 27925 emu Oe mol⁻¹ for an $S_{\text{tot}} = 2 + \frac{1}{2} = 5/2$ system. The reduced saturation observed in the present case may be attributed to spin canting in the system due to the single ion anisotropy of Mn^{III} .³⁷

The onset of higher dimensional ordering, *i.e.*, 2- and 3-D, was examined by the in-phase, $\chi'(T)$, and out-of-phase, $\chi''(T)$, components of the 10, 100, and 1000 Hz ac susceptibility, $\chi_{\text{ac}}(T)$, as shown in Fig. 6 for **1** (ESI, Fig. S6 for **2**). The peaks in the 10 Hz $\chi'(T)$ at 6.2 and 6.0 K for **1** and **2**, respectively, are a better measure of the ordering temperature, T_{c} . The peaks in the out-of-phase component, $\chi''(T)$, characteristic of a noncompensated moment, are present at 5.5 and 4.6 K for **1** and **2**, respectively. There are large frequency dependencies of

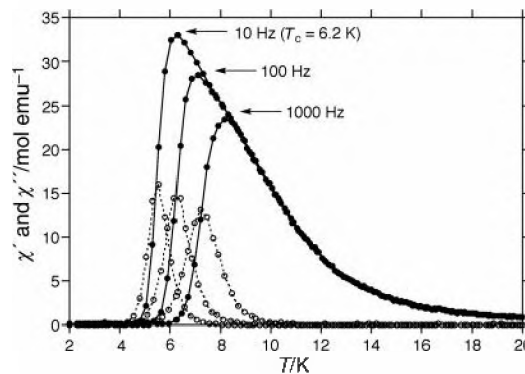


Fig. 6 In-phase, χ' (●) and out-of-phase, χ'' (○), components of the ac susceptibility at 10, 100, and 1000 Hz, respectively, for **1**.

both $\chi'(T)$ and $\chi''(T)$ for both **1** and **2**, which is characteristic of either a spin glass or a superparamagnetic state.⁴² Hysteresis with coercive fields of 17800 and 9600 Oe and remanent magnetizations, M_{r} , of 14400 and 10200 emu Oe mol⁻¹ are observed for **1** and **2** at 2 K, respectively. These values are smaller than those for $[\text{MnP}][\text{TCNE}]$ s, but they are still larger than those for other molecule-based and/or commercially used Fe_3O_4 magnets, 213 Oe.^{9a}

Conclusion

Two DCNQI-based magnets are reported that expand the utility of DCNQIs in materials other than molecule-based metals. The ETSSs **1** and **2** are the first structurally characterised monoanionic DCNQIs and the first coordinated ETSSs based on an early transition metal, and not copper,^{2,43} ruthenium,⁷ molybdenum,⁴⁴ silver,^{31,45} nor alkali metals.⁴⁵

The bulk magnetic ordering behaviour of the DCNQI-based ETSSs was also reported for the first time. Considering the coordination geometries and the exchange interactions, J , of **1** (-90 K) and **2** (-50 K), the orbital interaction between d_{z^2} of Mn^{III} and $p\pi^*$ of $[\text{TCNE}]^{\cdot-}$ is the most plausible exchange pathway, as suggested earlier.³⁶ It is well known that J is strongly dependent on the distances, R , *e.g.*, $|J| \propto A(R)\exp(-bR)$, where $A(R)$ is a polynomial in R and b is a constant.⁴⁶ The $d\text{Mn}-\text{Mn}$ values of **1** and **2** are ~ 3 Å longer than those of the corresponding $[\text{TCNE}]^{\cdot-}$ ETSSs due to the larger size of the DCNQIs, however, the exchange interactions of **1** and **2** are similar to those observed for $[\text{Mn}^{\text{III}}\text{P}]^+[\text{TCNE}]^{\cdot-}$ ETSSs. These large J values of **1** and **2** and the longer $d\text{Mn}-\text{Mn}$ values are consistent with the large atomic coefficient on the terminal nitrogens for $[\text{DCNQI}]^{\cdot-}$,⁴³ which produce essential $d_{z^2}-p\pi^*$ orbital interactions.^{16,36} Although the values of **1** and **2** are smaller than those observed for ruthenium-based DCNQI ETSSs (~ -575 K),⁸ which have strong $d_{z^2}-p\pi^*$ orbital interactions, the combination of $[\text{Mn}^{\text{III}}\text{P}]^+$ and $[\text{DCNQI}]^{\cdot-}$ is a good candidate for obtaining a magnet with enhanced physical properties. We are currently working on the modification of the substituents in the DCNQIs and the porphyrin ligand and metals of the porphyrin.

Experimental

p-Xylene (Nacalai Tesque, Inc.; >98%) and chlorobenzene (Wako Pure Chemical Ind., Ltd.; 98%) were distilled under nitrogen over sodium and CaH_2 , respectively. DCNQIs were prepared according to the reported method.²¹ Other reagents and solvents were used as received. All manipulations involving the handling of $\text{Mn}^{\text{II,III}}$ TMesPs were performed in a glove box with less than 1 ppm oxygen. Infrared spectra were recorded on a Perkin-Elmer System-2000 FT-IR in the range of 650 to 4000 cm^{-1} on NaCl discs as a mineral oil mull.

Table 3 Crystallographic data for **1**, **2**, and DMeO-DCNQI

	1	2	DMeO-DCNQI
Formula	C ₉₀ H ₉₀ MnN ₈ O ₇	C ₉₀ H ₈₀ Cl ₄ MnN ₈	C ₁₀ H ₈ N ₄ O ₂
<i>M_r</i> /Da	1370.69	1470.43	216.20
Crystal system	Triclinic	Monoclinic	Monoclinic
Space group	<i>P</i> ̄ (no. 2)	<i>P</i> 2 ₁ / <i>c</i> (no. 14)	<i>P</i> 2 ₁ / <i>c</i> (no. 14)
<i>a</i> /Å	12.795(2)	12.988(5)	4.716(2)
<i>b</i> /Å	14.082(2)	20.020(6)	16.583(2)
<i>c</i> /Å	12.042(2)	15.548(5)	6.709(2)
<i>α</i> /°	104.33(1)		
<i>β</i> /°	95.09(2)	104.60(3)	104.84(2)
<i>γ</i> /°	111.35(1)		
Volume/Å ³	1919.2(7)	3911(2)	507.2(2)
<i>Z</i>	1	2	2
<i>T</i> /K	223.0(4)	198.0(4)	224.0(4)
<i>ρ</i> _{calc} /g cm ⁻³	1.186	1.248	1.416
<i>μ</i> (Mo-Kα)/cm ⁻¹	2.26	3.56	1.04
<i>R</i> _w	0.085	0.165	0.078
<i>R</i> ₁	0.060	0.109	0.053

[Mn^{III}TMesP]⁺[DMeO-DCNQI]⁻, **1**

A filtered hot solution of [Mn^{II}TMesP]·pyridine (100.0 mg, 0.12 mmol) in 50 mL of boiling *p*-xylene was added to DMeO-DCNQI (50.0 mg, 0.23 mmol) in 50 mL of hot *p*-xylene. The solution was left to stand for two days at room temperature, to form black–green crystals, which were collected by vacuum filtration and dried under vacuum for 3 h (yield: 35.0 mg, 21%). Anal. for the stoichiometry of [Mn^{III}TMesP]⁺[DMeO-DCNQI]⁻·2*p*-xylene as calc. for C₈₂H₈₀MnN₈O₂: C, 77.89; H, 6.38; N, 8.86%. Found: C, 77.60; H, 6.16; N, 8.62%.

[Mn^{III}TMesP]⁺[DMe-DCNQI]⁻, **2**

A procedure similar to that described above was used for the synthesis of **2**, starting from 100.0 mg of Mn^{II}TMesP, 22.0 mg of DMe-DCNQI, and 100 mL of PhCl. This yielded 40.0 mg of **2** (23%). Some solvents are lost during the vacuum drying. Anal. for the stoichiometry of [Mn^{III}TMesP]⁺[DMe-DCNQI]⁻·3.72PhCl as calc. for C_{88.32}H_{78.60}Cl_{3.72}MnN₈: C, 73.73; H, 5.51; N, 7.79%. Found: C, 73.53; H, 5.83; N, 7.99%.

Crystallographic studies§

The crystal data of the complexes are summarised in Table 3. The temperature was calibrated with an Anritsu HFT-50 thermometer. Data for **1**, **2**, and MeO-DCNQI were collected on a Rigaku AFC7R four circle diffractometer system with a graphite monochromated Mo-Kα radiation (*λ* = 0.71070 Å, 60 kV, 300 mA) equipped with a Rigaku low temperature device. The data were collected using the *ω*-2*θ* scan technique.

Physical methods

The XPS were recorded on a KRATOS XSAM-800 equipped with a Mg anode X-ray gun (*hν* = 1253.6 eV). The spectrometer was directly connected to a dry box made in-house. The spectrometer was calibrated so that the Au 4f_{7/2} peak of the clean sputtered metals appeared at 84.0 eV and the ionisation potentials were reproducible to a precision of $\leq \pm 0.10$ eV. A detailed description of the conditions of the XPS measurements have been reported elsewhere.⁴⁷ The magnetic susceptibility between 2 and 300 K was determined on a Quantum Design MPMS-5XL 5 T SQUID (sensitivity = 10⁻⁸ emu or 10⁻¹² emu Oe⁻¹ at 1 T) magnetometer with ultra-low field (~0.005 Oe), and ac options using a reciprocating sample measurement system, and continuous low temperature control with enhanced thermometry features. The ac magnetic

susceptibility (*χ'* and *χ''*) was studied in the range of 10 to 1000 Hz. Samples were loaded in an airtight Delrin[®] holder and packed with oven-dried quartz wool (to prevent movement of the sample in the holder) or in a gelatine capsule. For isofield dc measurements, the samples were zero-field cooled (following oscillation of the dc field), and data collected upon warming. For dc isothermal and ac measurements, remanent fluxes were minimised by oscillation of the dc field, followed by quenching of the magnet. Remaining fluxes were detected using a flux gate gaussmeter and further minimised by application of an opposing field, to bring the dc field to <0.5 Oe. The diamagnetic corrections of -926 and -897 × 10⁻⁶ emu mol⁻¹ were used for [Mn^{III}TMesP][DMeO-DCNQI], **1**, and [Mn^{III}TMesP][DMe-DCNQI], **2**, respectively.

Acknowledgements

This paper is dedicated to the memory of the late Mrs Fusako Fukuda, the Materials Analysis Centre of ISIR, Osaka University, and to her helpful technical support. This work was supported in part by Grants-in-Aid for Scientific Research on Priority Area (#12023226 “Metal-assembled Complexes” to K.-i.S., #12042250 “Molecular Physical Chemistry” to K.-i.S., #10146103 “Creation of Characteristic Delocalized Electronic Systems” to Y.S., COE Research to Y.S., as well as #12440178 to K.-i.S. and #12440199 to Y.S.) from the Ministry of Education, Science, Sports and Culture, Japan, a *Basic Research 21 for Breakthroughs in Info-communications* (to K.-i.S.) from the Ministry of Posts and Telecommunications, and US NSF Grant No. CHE-9320478 to J.S.M. This research was also financially supported by grants from the Izumi Science & Technology Foundation (to K.-i.S.) and the Sumitomo Foundation (to K.-i.S.). We appreciate the technical assistance provided by the Materials Analysis Centre of ISIR, Osaka University, Mr N. Miyazaki, Chiba University as well as helpful discussions with Dr Satoshi Takara, ISIR, Osaka University.

References

- 1 A. Aumüller and S. Hünig, *Angew. Chem., Int. Ed. Engl.*, 1984, **23**, 447.
- 2 Reviews: (a) S. Hünig, *J. Mater. Chem.*, 1995, **5**, 1469; (b) P. Erk, H. Meixner, T. Metzenthin, S. Hünig, U. Langohr, J. U. von Schütz, H.-P. Werner, H. C. Wolf, R. Burkert, H. W. Helberg and G. Schaumburg, *Adv. Mater.*, 1991, **3**, 311; (c) S. Hünig and P. Erk, *Adv. Mater.*, 1991, **3**, 225; (d) S. Hünig, *Pure Appl. Chem.*, 1990, **62**, 395.
- 3 (a) S. Hünig, K. Sinzger and M. Jopp, *Angew. Chem., Int. Ed. Engl.*, 1992, **31**, 859; (b) K. Sinzger, S. Hünig, M. Jopp, D. Bauer, W. Bietsch, J. U. von Schütz, H. C. Wolf, R. K. Kremer, T. Metzenthin, R. Bau, S. I. Khan, A. Lindbaum, C. L. Lengauer and E. Tillmanns, *J. Am. Chem. Soc.*, 1993, **115**, 7696.
- 4 S. Uji, T. Terashima, H. Aoki, J. S. Brooks, K. Kato, H. Sawa, S. Aonuma, M. Tamura and M. Kinoshita, *Phys. Rev.*, 1994, **B50**, 15597.
- 5 H. Kobayashi, A. Kobayashi and P. Cassoux, *Chem. Soc. Rev.*, 2000, **29**, 325.
- 6 J. S. Miller, C. Vazquez, R. S. McLean, W. M. Reiff, A. Aumüller and S. Hünig, *Adv. Mater.*, 1993, **5**, 448.
- 7 Reviews: (a) R. J. Crutchley, *Adv. Inorg. Chem.*, 1994, **41**, 273; (b) W. Kaim, A. Klein and M. Glöckle, *Acc. Chem. Res.*, 2000, **33**, 755.
- 8 M. A. S. Aquino, F. L. Lee, E. J. Gabe, C. Bensimon and J. E. Greedan, *J. Am. Chem. Soc.*, 1992, **114**, 5130.
- 9 Reviews: (a) J. S. Miller and A. J. Epstein, *Angew. Chem., Int. Ed. Engl.*, 1994, **33**, 385; (b) J. S. Miller and A. J. Epstein, *Chem. Commun.*, 1998, 1319; (c) J. S. Miller, *Inorg. Chem.*, 2000, **39**, 4392.
- 10 K.-i. Sugiura, S. Mikami, M. T. Johnson, J. S. Miller, K. Iwasaki, K. Umishita, S. Hino and Y. Sakata, *Chem. Lett.*, 1999, 925.
- 11 K.-i. Sugiura, S. Mikami, M. T. Johnson, J. S. Miller, K. Iwasaki, K. Umishita, S. Hino and Y. Sakata, *J. Mater. Chem.*, 2000, **10**, 959.

§CCDC reference numbers 138303–138305. See <http://www.rsc.org/suppdata/jm/b1/b100936m/> for crystallographic files in .cif or other electronic format.

- 12 M. T. Johnson, A. M. Arif and J. S. Miller, *Eur. J. Inorg. Chem.*, 2000, 1781.
- 13 J. S. Miller, C. Vazquez, N. L. Jones, R. S. McLean and A. J. Epstein, *J. Mater. Chem.*, 1995, **5**, 707.
- 14 C. M. Wynn, M. A. Girtu, J. S. Miller and A. J. Epstein, *Phys. Rev. B: Condens. Matter*, 1997, **56**, 315.
- 15 C. M. Wynn, M. A. Girtu, J. S. Miller and A. J. Epstein, *Phys. Rev. B: Condens. Matter*, 1997, **56**, 14050.
- 16 K.-i. Sugiura, A. M. Arif, D. K. Rittenberg, J. Schweizer, L. Öhrstrom, A. J. Epstein and J. S. Miller, *Chem. Eur. J.*, 1997, **3**, 138.
- 17 D. K. Rittenberg, K.-i. Sugiura, A. M. Arif, Y. Sakata, C. D. Incarvito, A. L. Rheingold and J. S. Miller, *Chem. Eur. J.*, 2000, **6**, 1811.
- 18 D. K. Rittenberg and J. S. Miller, *Inorg. Chem.*, 1999, **38**, 4838.
- 19 D. K. Rittenberg, K.-i. Sugiura, Y. Sakata, S. Mikami, A. J. Epstein and J. S. Miller, *Adv. Mater.*, 2000, **12**, 126.
- 20 (a) E. J. Brandon, G. P. A. Yap, A. L. Rheingold, A. Arif and J. S. Miller, *Inorg. Chim. Acta*, 1995, **240**, 515; (b) K.-i. Sugiura, S. Mikami, T. Tanaka, M. Sawada and Y. Sakata, *Chem. Lett.*, 1998, 103; (c) M. L. Yates, A. M. Arif, J. L. Manson, B. A. Kalm, B. M. Burkhardt and J. S. Miller, *Inorg. Chem.*, 1998, **37**, 840; (d) S. Mikami, K.-i. Sugiura, J. S. Miller and Y. Sakata, *Chem. Lett.*, 1999, 413.
- 21 A. Aumüller and S. Hünig, *Liebigs Ann. Chem.*, 1986, 142.
- 22 S. Hünig, T. Metzenthin, K. Peters, J.-U. von Schütz and H. G. von Schnering, *Eur. J. Org. Chem.*, 1998, 1653.
- 23 G. Lunardi and C. Pecile, *J. Chem. Phys.*, 1991, **95**, 6911.
- 24 A. Aumüller, E. Peter, S. Hünig, H. Meixner, J.-U. von Schütz and H.-P. Werner, *Liebigs Ann. Chem.*, 1987, 997.
- 25 A. Aumüller, P. Erk, S. Hünig, E. Hädicke, K. Peters and H. G. von Schnering, *Chem. Ber.*, 1991, **124**, 2001.
- 26 L. L. Cheruiyot, L. K. Thompson, J. E. Greedan, G. Liu and R. J. Crutchley, *Can. J. Chem.*, 1995, **73**, 573.
- 27 K. Nakamoto, in *Infrared and Raman Spectra of Inorganic and Coordination Compounds 5th Edition (Part B)*, John Wiley & Sons, New York, 1997, p. 113.
- 28 A. Johnson and H. Taube, *J. Indian Chem. Soc.*, 1989, **66**, 503.
- 29 (a) H. Kobayashi, A. Miyamoto, H. Moriyama, R. Kato and A. Kobayashi, *Chem. Lett.*, 1991, 863; (b) Y. Yamakita, Y. Furukawa, A. Kobayashi, M. Tasumi, R. Kato and H. Kobayashi, *J. Chem. Phys.*, 1994, **100**, 2449; (c) S. Aoki and T. Nakayama, *Phys. Rev. B: Condens. Matter*, 1997, **56**, R2893; (d) S. Basaki and S. Matsuzaki, *Solid State Commun.*, 1994, **91**, 865.
- 30 K.-i. Sugiura, S. Mikami, K. Iwasaki, S. Hino, E. Asato and Y. Sakata, *J. Mater. Chem.*, 2000, **10**, 315.
- 31 T. Mori and H. Inokuchi, *Chem. Lett.*, 1990, 2077.
- 32 J. S. Miller, C. Vazquez, J. C. Calabrese, R. S. Mclean and A. J. Epstein, *Adv. Mater.*, 1994, **6**, 217.
- 33 (a) R. Kato, H. Kobayashi and A. Kobayashi, *J. Am. Chem. Soc.*, 1989, **111**, 5224; (b) K. Sinzger, S. Hünig, M. Jopp, D. Bauer, W. Bietsch, J. U. von Schütz, H. C. Wolf, R. K. Kremer, T. Metzenthin, R. Bau, S. I. Khan, A. Lindbaum, C. L. Lengauer and E. Tillmanns, *J. Am. Chem. Soc.*, 1993, **115**, 7696.
- 34 C. E. B. Evans, G. P. A. Yap and R. J. Crutchley, *Inorg. Chem.*, 1998, **37**, 6161.
- 35 A. R. Rezvani, C. Bensimon, B. Crompt, C. Reber, J. E. Greedan, V. V. Kondratiev and R. J. Crutchley, *Inorg. Chem.*, 1997, **36**, 3322.
- 36 E. J. Brandon, C. Kollmar and J. S. Miller, *J. Am. Chem. Soc.*, 1998, **120**, 1822.
- 37 C. M. Wynn, M. A. Giryu, W. B. Brinckerhoff, K.-i. Sugiura, J. S. Miller and A. J. Epstein, *Chem. Mater.*, 1997, **9**, 2156.
- 38 (a) E. J. Brandon, K.-i. Sugiura, A. M. Arif, L. Liable-Sands, A. L. Rheingold and J. S. Miller, *Mol. Cryst. Liq. Cryst.*, 1997, **305**, 269; (b) E. J. Brandon, A. M. Arif, J. S. Miller, K.-i. Sugiura and B. M. Burkhardt, *Cryst. Eng.*, 1998, **1**, 97; (c) K.-i. Sugiura, A. M. Arif and J. S. Miller, manuscript in preparation.
- 39 *Out-of-registry* refers to parallel chains with D's near A's and A's near D's, and *in-registry* refers to the chain with D's near D's and A's near D's.
- 40 (a) E. Coronado, M. Drillon and R. Georges, in *Research Frontiers in Magnetochemistry*, ed. C. J. O'Connor, World Scientific, 1993, p. 26; (b) D. Beltran, M. Drillon, E. Coronado and R. Georges, *Stud. Inorg. Chem.*, 1983, **3**, 583; (c) M. Drillon, E. Coronado, D. Beltran and R. Georges, *Chem. Phys.*, 1983, **79**, 449; (d) M. Verdager, M. Julve, A. Michalowicz and O. Kahn, *Inorg. Chem.*, 1983, **22**, 2624; (e) M. Drillon, J. C. Gianduzzo and R. Georges, *Phys. Lett.*, 1983, **96A**, 413.
- 41 J. Seiden, *J. Phys. Lett.*, 1983, **44**, L947.
- 42 J. Mydosh, *Spin Glasses*. Taylor and Francis, Washington, DC, 1993.
- 43 H. Oshio, *Inorg. Chem.*, 1993, **32**, 4123.
- 44 X. Ouyang, C. Campana and K. R. Dunbar, *Inorg. Chem.*, 1996, **35**, 7188.
- 45 R. Kato, H. Kobayashi, A. Kobayashi, T. Mori and H. Inokuchi, *Chem. Lett.*, 1987, 1579.
- 46 R. E. Coffman and G. R. Buettner, *J. Phys. Chem.*, 1979, **83**, 2387.
- 47 S. Hino, K. Umishita, K. Iwasaki, K. Tanaka, T. Sato, T. Yamabe, K. Yoshizawa and K. Okahara, *J. Phys. Chem. A*, 1997, **101**, 4346.
- 48 M. A. S. Aquino, R. J. Crutchley, F. L. Lee, E. J. Gabe and C. Bensimon, *Acta Crystallogr., Sect. C: Cryst. Struct. Commun.*, 1993, **49**, 1543.